An atmospheric radiation model for the Very Large Telescope at Cerro Paranal in Chile

S. Noll (stefan.noll@uibk.ac.at)**, W. Kausch, M. Barden, A.M. Jones, C. Szyszka, and S. Kimeswenger**
Institute for Astro- and Particle Physics, University of Innsbruck

Motivation:

The quality of ground-based astronomical observations is strongly affected by scattering, absorption, and radiation processes in the Earth's atmosphere. For effective telescope time management, it is important to accurately estimate the wavelength-dependent contribution of the Earth's atmosphere to the observed flux. For this reason, we developed an atmospheric radiation model (Fig. A) for the Very Large Telescope of the European Southern Observatory at Cerro Paranal (2635 m) in Chile's Atacama desert.

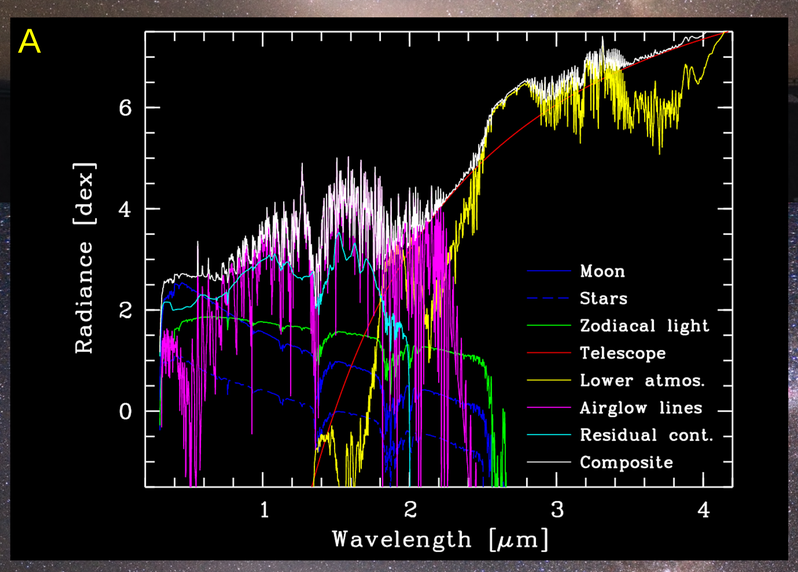

(A) Model components for wavelengths between 0.3 and 4.2 μm and logarithmic radiance units. This example, with the Moon above the horizon, shows scattered moonlight, scattered starlight, zodiacal light, thermal telescope emission, molecular emission of the lower atmosphere, airglow emission lines of the upper atmosphere, and airglow/residual continuum.

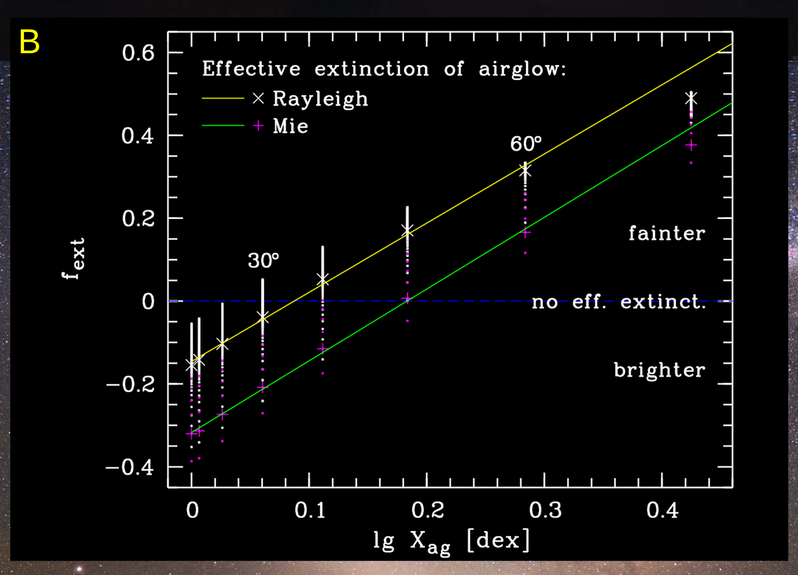

(B) Deviation of airglow intensity from van Rhijn intensity (X_{ag} = I(z) /I_0 for layer at 90 km) by atmospheric extinction as derived from 3D scattering calculations. The factor f_{ext} (= 0 for van Rhijn case) is related to the effective optical depth by $\tau_{eff} = f_{ext}\ \tau_0\ X_{ag}$. For Rayleigh scattering by molecules and Mie scattering by aerosols, the dots show results for different zenith distances z and zenithal optical depths τ_0. The lines indicate the relations used in our model.

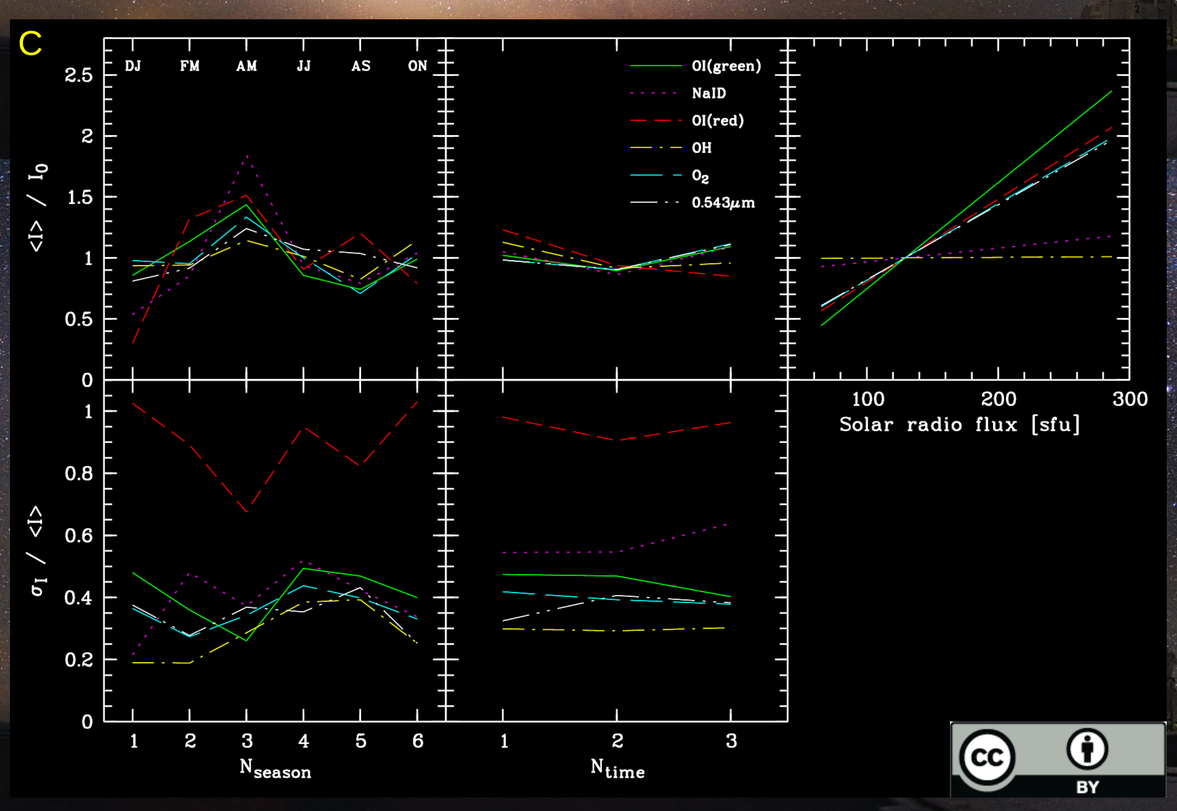

(C) Variability correction for the five airglow line classes green OI, NaID, red OI, OH, and O_2, and the airglow continuum (analysed at 543 nm). *Upper panels*: The variability depends on bimonthly period (1 = Dec/Jan,..., 6 = Oct/Nov), time bin (third of the night), and solar activity measured by the solar radio flux. *Lower panels*: For seasonal period and time, the relative uncertainties of the variability correction are shown as well.

Model features:

- Wavelength coverage from 0.3 to 30 μm
- Atmospheric extinction includes Rayleigh scattering, aerosol extinction (Patat et al. 2011, A&A 527), and molecular absorption
- Absorption and emission in the lower atmosphere is calculated by the radiative transfer code LBLRTM (Clough et al. 2005, JQSRT 91) for atmospheric profiles dependent on season and zenith distance
- 3D single scattering calculations with a multiple scattering correction were performed to derive relations for estimating the effective extinction of extended emission sources like zodiacal light and airglow (Fig. B)
- Spectroscopic extension and optimisation of the Krisciunas & Schaefer (1991, PASP 103) model for scattered moonlight in the V band
- Mean spectrum of scattered starlight
- Zodiacal light model based on Leinert et al. (1998, A&AS 127)
- Thermal telescope emission modelled as grey bodies
- Airglow line list based on Cosby et al. (2006, J. Geophys. Res. 111) atlas, OH calculations of Rousselot et al. (2000, A&A 354), and HITRAN database (Rothman et al. 2009, JQSRT 110)
- Airglow intensity and variability were derived from 1186 optical FORS1 spectra taken over 6 years (Patat 2008, A&A 481)
- Airglow intensity dependent on zenith distance, solar radio flux, bimonthly period, third of the night, and variability class (green OI, NaID, red OI, OH, O_2, and continuum at 543 nm) (Fig. C)
- Mean airglow/residual continuum scaled to intensity at 543 nm (Fig. D)

Quality:

A comparison of the resulting model with observed photometric and spectroscopic data yields an accuracy of about 20 per cent (Fig. E), which is a significant improvement over previous models for Cerro Paranal.

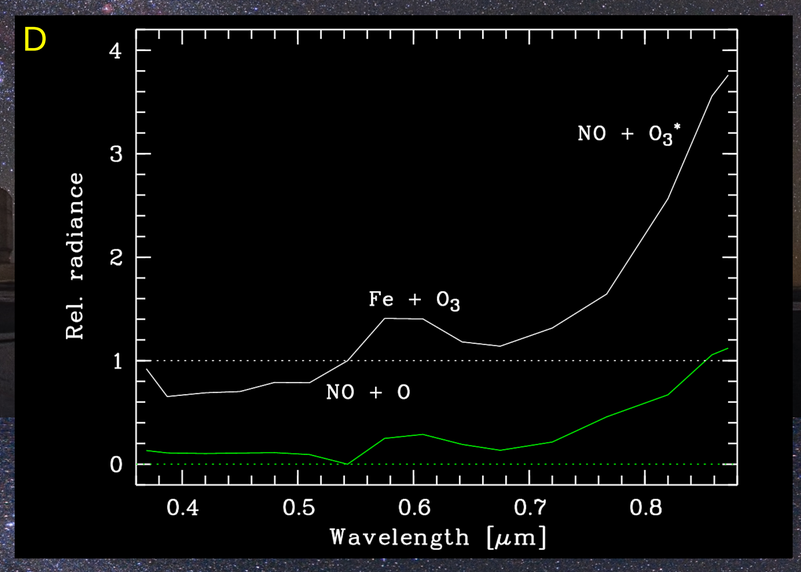

(D) Optical airglow continuum (white) and its variability (green) relative to the reference wavelength 543 nm. The most probable chemical reactions for the different continuum components are indicated. The nitric oxide continua show distinctly broader wavelength distributions than the iron-related pseudo continuum.

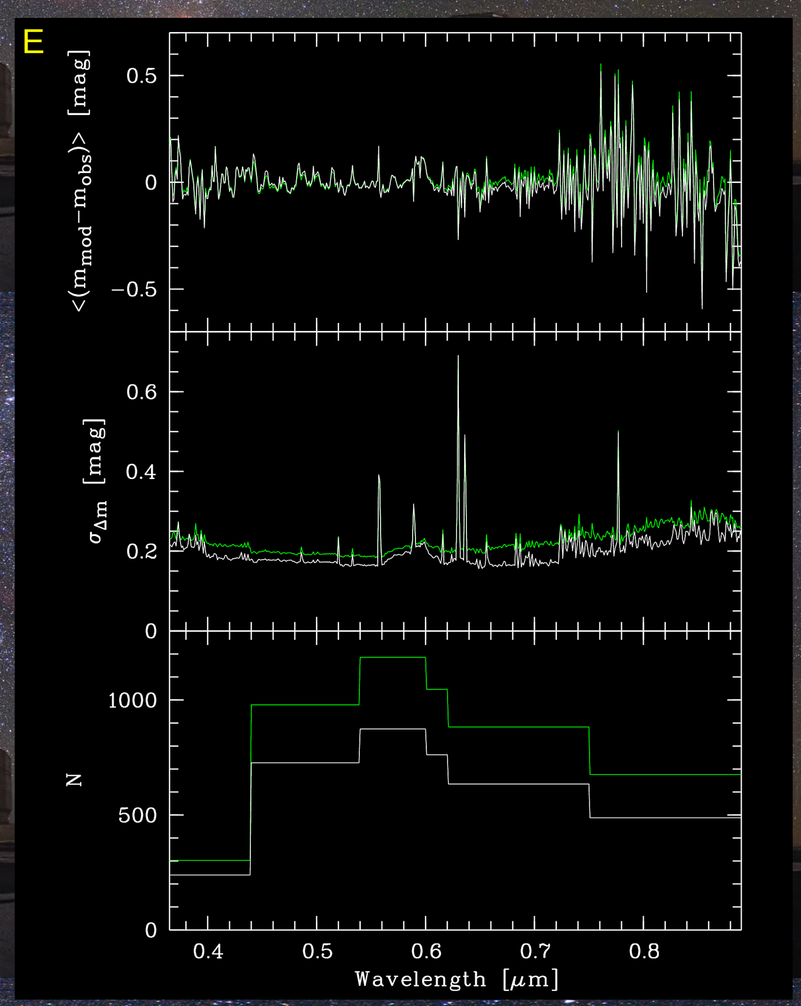

(E) Deviations between our model and the FORS1 spectra of Patat (2008) in magnitudes. The mean magnitude difference (*upper panel*), the standard deviation (*middle panel*), and the wavelength-dependent number of considered spectra (*lower panel*) are shown for 1 nm bins. Results for the full spectroscopic data set (green) and for spectra with the Moon below the horizon (white) are displayed.

CC BY

funded by BMWF

Image: ESO/Y. Beletsky